Testing ultrafast mode-locking at microhertz relative optical linewidth

Michael J. Martin[1,*], **Seth M. Foreman**[1,2], **T. R. Schibli**[1], **and Jun Ye**[1]

[1] *JILA, National Institute of Standards and Technology and University of Colorado Department of Physics, University of Colorado, Boulder, CO 80309–0440*

[2] *Current address: Varian Physics, Room 246, 382 Via Pueblo Mall, Stanford, CA 94305-4060*

[*] Corresponding author: *Michael.J.Martin@colorado.edu*

Abstract: We report new limits on the phase coherence of the ultrafast mode-locking process in an octave-spanning Ti:sapphire comb. We find that the mode-locking mechanism correlates optical phase across a full optical octave with less than 2.5 μHz relative linewidth. This result is at least two orders of magnitude below recent predictions for quantum-limited individual comb-mode linewidths, verifying that the mode-locking mechanism strongly correlates quantum noise across the comb spectrum.

OCIS codes: (320.7090) Ultrafast lasers; (120.3940) Metrology; (140.4050) Mode-locked lasers.

References and links

1. T. Udem, R. Holzwarth, and T. W. Hänsch, "Optical frequency metrology," Nature **416**, 233–237 (2002).
2. S. T. Cundiff and J. Ye, "Colloquium: Femtosecond optical frequency combs," Rev. Mod. Phys. **75**, 325–342 (2003).
3. W. H. Oskay, S. A. Diddams, E. A. Donley, T. M. Fortier, T. P. Heavner, L. Hollberg, W. M. Itano, S. R. Jefferts, M. J. Delaney, K. Kim, F. Levi, T. E. Parler, and J. C. Begquist, "Single-Atom Optical Clock with High Accuracy," Phys. Rev. Lett. **97**, 020801 (2006).
4. H. S. Margolis, G. P. Barwood, G. Huang, H. A. Klein, S. N. Lea, K. Szymaniec, and P. Gill, "Hertz-Level Measurement of the Optical Clock Frequency in a Single $^{88}Sr^{+}$ Ion," Science **306**, 1355–1358 (2004).
5. A. A. Madej, J. E. Bernard, P. Dubé, L. Marmet, and R. S. Windeler, "Absolute frequency of the $^{88}Sr^{+}$ $5s^2S_{1/2}$–$4d^2D_{5/2}$ reference transition at 445 THz and evaluation of systematic shifts," Phys. Rev. A **70**, 012507 (2004).
6. T. Rosenband, D. B. Hume, P. O. Schmidt, C. W. Chou, A. Brusch, L. Lorini, W. H. Oskay, R. E. Drullinger, T. M. Fortier, J. E. Stalnaker, S. A. Diddams, W. C. Swann, N. R. Newbury, W. M. Itano, D. J. Wineland, and J. C. Bergquist, "Frequency Ratio of Al^{+} and Hg^{+} Single-Ion Optical Clocks; Metrology at the 17th Decimal Place," Science **319**, 1808–1812 (2008).
7. A. D. Ludlow, T. Zelevinsky, G. K. Campbell, S. Blatt, M. M. Boyd, M. H. G. de Miranda, M. J. Martin, J. W. Thomsen, S. M. Foreman, J. Ye, T. M. Fortier, J. E. Stalnaker, S. A. Diddams, Y. Le Coq, Z. W. Barber, N. Poli, N. D. Lemke, K. M. Beck, and C. W. Oates, "Sr lattice clock at 1×10^{-16} fractional uncertainty by remote optical evaluation with a Ca clock," Science **319**, 1805–1808 (2008).
8. N. Poli, Z. W. Barber, N. D. Lemke, C. W. Oates, L.-S. Ma, J. E. Stalnaker, T. M. Fortier, S. A. Diddams, L. Hollberg, J. C. Bergquist, A. Brusch, S. Jefferts, T. Heavner, and T. Parker, "Frequency evaluation of the doubly forbidden $^1S_0$–$^3P_0$ transition in bosonic ^{174}Yb," Phys. Rev. A **77**, 050501 (2008).
9. M. Takamoto, F.-L. Hong, R. Higashi, and H. Katori, "An optical lattice clock," Nature **435**, 321–324 (2005).
10. U. Sterr and C. Degenhardt and H. Stoehr and C. Lisdat and H. Schnatz and J. Helmcke and F. Riehle and G. Wilpers and C. Oates and L. Hollberg, "The optical calcium frequency standards of PTB and NIST," Comptes Rendus Physique **5**, 845–855 (2004).
11. A. D. Ludlow, M. M. Boyd, T. Zelevinsky, S. M. Foreman, S. Blatt, M. Notcutt, T. Ido, and J. Ye, "Systematic Study of the ^{87}Sr Clock Transition in an Optical Lattice," Phys. Rev. Lett. **96**, 033003 (2006).
12. R. Le Targat, X. Baillard, M. Fouché, A. Brusch, O. Tcherbakoff, G. D. Rovera, and P. Lemonde, "Accurate Optical Lattice Clock with ^{87}Sr Atoms," Phys. Rev. Lett. **97**, 130801 (2006).
13. G. K. Campbell, A. D. Ludlow, S. Blatt, J. W. Thomsen, M. J. Martin, M. H. G. Miranda, T. Zelevinsky, M. M. Boyd, J. Ye, S. A. Diddams, T. P. Heavner, T. E. Parker, and S. R. Jefferts, "The absolute frequency of the ^{87}Sr optical clock transition," Metrologia **45**, 539–548 (2008).

#102990 - $15.00 USD Received 22 Oct 2008; revised 4 Dec 2008; accepted 12 Dec 2008; published 7 Jan 2009

14. K.-K. Ni, S. Ospelkaus, M. H. G. de Miranda, A. Pe'er, B. Neyenhuis, J. J. Zirbel, S. Kotochigova, P. S. Julienne, D. S. Jin, and J. Ye, "A High Phase-Space-Density Gas of Polar Molecules," Science **322**, 231–235 (2008).
15. J. G. Danzl, E. Haller, M. Gustavsson, M. J. Mark, R. Hart, N. Bouloufa, O. Dulieu, H. Ritsch, and H.-C. Nagerl, "Quantum Gas of Deeply Bound Ground State Molecules," Science **321**, 1062–1066 (2008).
16. L. S. Ma, Z. Bi, A. Bartels, L. Robertsson, M. Zucco, R. S. Windeler, G. Wilpers, C. Oates, L. Hollberg, and S. A. Diddams, "Optical Frequency Synthesis and Comparison with Uncertainty at the 10^{-19} Level," Science **303**, 1843–1845 (2004).
17. L.-S. Ma, Z. Bi, A. Bartels, K. Kim, L. Robertsson, M. Zucco, R. S. Windeler, G. Wilpers, C. Oates, L. Hollberg, and S. A. Diddams, "Frequency Uncertainty for Optically Referenced Femtosecond Laser Frequency Combs," IEEE J. Quantum Electron. **43**, 139–146 (2007).
18. A. Bartels, C. W. Oates, L. Hollberg, and S. A. Diddams, "Stabilization of femtosecond laser frequency combs with subhertz residual linewidths," Opt. Lett. **29**, 1081–1083 (2004).
19. J. Stenger, H. Schnatz, C. Tamm, and H. R. Telle, "Ultraprecise Measurement of Optical Frequency Ratios," Phys. Rev. Lett. **88**, 073601 (2002).
20. T. R. Schibli, I. Hartl, D. C. Yost, M. J. Martin, A. Marcinkevi, M. E. Fermann, and J. Ye, "Optical frequency comb with submillihertz linewidth and more than 10 W average power," Nature Photonics **2**, 355–359 (2008).
21. D. J. Jones, S. A. Diddams, J. K. Ranka, A. Stentz, R. S. Windeler, J. L. Hall, and S. T. Cundiff, "Carrier-Envelope Phase Control of Femtosecond Mode-Locked Lasers and Direct Optical Frequency Synthesis," Science **288**, 635–639 (2000).
22. J. Reichert, R. Holzwarth, T. Udem, and T. W. Hänsch, "Measuring the frequency of light with mode-locked lasers," Opt. Commun. **172**, 59–68 (1999).
23. J. Ye, J. L. Hall, and S. A. Diddams, "Precision phase control of an ultrawide-bandwidth femtosecond laser: a network of ultrastable frequency marks across the visible spectrum," Opt. Lett. **25**, 1675–1677 (2000).
24. T. M. Fortier, D. J. Jones, and S. T. Cundiff, "Phase stabilization of an octave-spanning Ti:sapphire laser," Opt. Lett. **28**, 2198–2200 (2003).
25. T. M. Fortier, J. Ye, S. T. Cundiff, and R. S. Windeler, "Nonlinear phase noise generated in air-silica microstructure fiber and its effect on carrier-envelope phase," Opt. Lett. **27**, 445–447 (2002).
26. A. L. Schawlow and C. H. Townes, "Infrared and Optical Masers," Phys. Rev. **112**, 1940–1949 (1958).
27. P. Goldberg, P. W. Milonni, and B. Sundaram, "Theory of the fundamental laser linewidth," Phys. Rev. A **44**, 1969–1985 (1991).
28. R. Paschotta, "Noise of mode-locked lasers (Part II): timing jitter and other fluctuations," Appl. Phys. B **79**, 163–173 (2004).
29. R. Paschotta, A. Schlatter, S. C. Zeller, H. R. Telle, and U. Keller, "Optical phase noise and carrier-envelope offset noise of mode-locked lasers," Appl. Phys. B **82**, 265–273 (2006).
30. F. X. Kärtner, U. Morgner, T. Schibli, R. Ell, H. A. Haus, J. G. Fujimoto, and E. P. Ippen, "Few-Cycle pulses directly from a laser," in *Few-cycle laser pulse generation and its applications*, F. X. Kärtner, ed., Topics in Appl. Phys. **95**, 73–135 (Springer–Verlag Berlin, 2004).
31. J. K. Wahlstrand, J. T. Willits, C. R. Menyuk, and S. T. Cundiff, "The quantum-limited comb lineshape of a mode-locked laser: Fundamental limits on frequency uncertainty," Opt. Express **16**, 18624–18630 (2008).

1. Introduction

Optical frequency combs have become ubiquitous tools for precision optical measurement [1, 2]. They have enabled a new generation of optical frequency references based on narrow transitions in single trapped ions [3–6] and cold, neutral, atomic ensembles [7–13]. In addition, the comb's ability to phase coherently transfer optical references across large spectral gaps allows for direct optical atomic clock comparison, placing new constraints on the evolution of fundamental constants [6] as well as driving atomic clock technology [7]. Recently, this broadband phase coherence has facilitated the production of ground-state ultracold polar molecules via stimulated Raman adiabatic passage [14, 15].

Previous evaluations have proven the frequency comb's suitability for precision optical metrology. The fractional frequency uncertainty of Ti:sapphire-based frequency combs has been evaluated at the 10^{-19} level at 1000 s [16, 17]. Experiments testing the phase coherence of Ti:sapphire combs have been able to place upper limits on the relative linewidth of different spectral regions for both locked and free running combs at 20 mHz [18] and 9 mHz [19], respectively, and were ultimately limited by by differential-path technical noise caused by air currents and mirror vibrations. The frequency comb used in this work was previously compared

#102990 - $15.00 USD Received 22 Oct 2008; revised 4 Dec 2008; accepted 12 Dec 2008; published 7 Jan 2009

to a 10 W average power Yb fiber comb locked to a common optical reference, with a resulting 1 mHz resolution bandwidth-limited relative linewidth [20]. This indicates that the Ti:Sapphire comb should be capable of supporting narrower relative linewidths. Here we report a new lower limit to the intrinsic phase coherence of a mode-locked Ti:sapphire laser phase locked to an optical reference, by both linewidth and phase noise measurements. This work demonstrates that the mode-locking process correlates the phase noise of individual frequency comb modes at a level far below the quantum noise limit of individual free-running comb modes.

A complete description of the frequency of a given output mode of a comb is given by

$$\nu_n(t) = n f_{\mathrm{rep}}(t) + f_0(t) + \varepsilon_n(t). \tag{1}$$

Here n is the index labeling the harmonic of the repetition rate $f_{\mathrm{rep}}(t)$ and $f_0(t)$ is the carrier envelope offset frequency. Both $f_{\mathrm{rep}}(t)$ and $f_0(t)$ are radio frequency (RF) signals that can be measured by directly observing the output pulse on a photodetector, and by employing a self-referencing technique (*e.g.* [21]), respectively. The term $\varepsilon_n(t)$ represents frequency noise in the vicinity of mode n that is not described by fluctuations in $f_{\mathrm{rep}}(t)$ or $f_0(t)$. In other words, $\varepsilon_n(t)$ accounts for mode-dependent noise terms that are at least quadratic in order with respect to n as a result of pulse-to-pulse fluctuations, which could be in part caused by time-dependent fluctuations of higher-order intracavity dispersion. Additionally, and most importantly, $\varepsilon_n(t)$ is also assumed to include fluctuations not related to any other comb mode—fluctuations that are completely uncorrelated across the comb. In this way, $\varepsilon_n(t)$ also accounts for possible spontaneous emission-induced frequency noise that does not affect the global timing and phase parameters of the comb as a result of imperfect mode-locking. This is in contrast to the case of an ideal comb, where the mode n is perfectly defined with respect to mode m in the limit where both ε_m and ε_n are zero, due to the mode locking mechanism enforcing a fixed phase relation across the comb. While the relative coherence of comb teeth is only limited by the quality of the mode-locking process, a free-running frequency comb, when compared to an external reference, has noise properties dominated by vibrational noise in the mirror mounts and thermal drifts in the laser cavity coupling to both f_{rep} and f_0.

Actively phase locking a Ti:sapphire comb to an optical reference requires control of both f_{rep} and f_0 via control of the laser cavity length and pulse group delay (*e.g.* [22, 23]). Combining the comb and a continuous wave (CW) laser results in a time-dependent heterodyne beat, formed when a given comb tooth n interferes with the CW laser. This RF signal is denoted by $f_{b,n}(t)$. By phase locking $f_{b,n}(t)$ to an RF source, the comb ideally acquires the optical phase information of the reference laser and the RF source. This is due to the fixed phase relationship between the comb's output modes, enforced by the mode-locking process. When locked via control of f_{rep}, $f_{b,n}(t)$ is related to the RF reference frequency, f_{RF}, and the comb degrees of freedom by

$$f_{b,n}(t) = f_{\mathrm{RF}} + \delta f_{b,n}(t) = n f_{\mathrm{rep}}(t) + f_0(t) + \varepsilon_n(t) - \nu_{\mathrm{CW}}(t). \tag{2}$$

Here, $\delta f_{b,n}(t)$ is the locking error due to the finite gain of the servo, and $\nu_{\mathrm{CW}}(t)$ is the frequency of the CW optical reference. We defer consideration of shot noise, which adds a white phase noise term to the right side of Eq. (2), to Section 3. Additionally locking f_0 to an RF reference, with locking error $\delta f_0(t)$, constrains both comb degrees of freedom. Solving for $f_{\mathrm{rep}}(t)$ yields

$$f_{\mathrm{rep}}(t) = \frac{1}{n}\left[f_{\mathrm{RF}} + \delta f_{b,n}(t) - \varepsilon_n(t) + \nu_{\mathrm{CW}}(t) - f_0 - \delta f_0(t)\right]. \tag{3}$$

It is important to note that the locking errors and noise term $\varepsilon_n(t)$ write noise onto $f_{\mathrm{rep}}(t)$, thus globally affecting the comb. Using Eq. (1) and $f_{\mathrm{rep}}(t)$ given in Eq. (3), the optical frequency of a comb mode numbered m is given by

$$\nu_m = \frac{m}{n}\left[f_{\mathrm{RF}} + \delta f_{b,n}(t) - \varepsilon_n(t) + \nu_{\mathrm{CW}}(t)\right] + \left(1 - \frac{m}{n}\right)\left[f_0 + \delta f_0(t)\right] + \varepsilon_m(t). \tag{4}$$

#102990 - $15.00 USD Received 22 Oct 2008; revised 4 Dec 2008; accepted 12 Dec 2008; published 7 Jan 2009

Again the added noise term, $\varepsilon_m(t)$, represents extra frequency noise added to mode m by both correlated and uncorrelated laser dynamics. Thus, measuring the comb mode m relative to mode n in a precise way allows upper limits on the intrinsic noise properties of the comb to be determined. One way to accomplish this, as we report in this work, is to use the second harmonic of the optical reference to which mode n is locked to compare the phase coherence of comb modes n and $m = 2n$ in a direct way. In this case, the expected heterodyne beat between the second harmonic light and the comb mode $2n$, which represents an out-of-loop measurement of the relative coherence of modes n and $2n$, is given by

$$f_{b,2n}(t) = \nu_{2n}(t) - 2\nu_{\mathrm{CW}}(t) = 2f_{\mathrm{RF}} - f_0 - \delta f_0(t) + 2\delta f_{b,n}(t) + \varepsilon_{2n}(t) - 2\varepsilon_n(t). \quad (5)$$

Here, the term $\varepsilon_{2n}(t) - 2\varepsilon_n(t)$ represents the time-fluctuating out-of-loop frequency noise added by the comb dynamics.

The Wiener–Khinchin theorem relates time-domain frequency fluctuations to single-sided frequency noise power spectral density by

$$S_\nu(f) = 4\int_0^\infty \cos(2\pi\tau f) R_{\xi\xi}(\tau) d\tau. \quad (6)$$

Here, $S_\nu(f)$ is the power spectral density associated with the time-fluctuating frequency $\xi(t)$. The autocorrelation term $R_{\xi\xi}(\tau)$ is defined by

$$R_{\xi\xi}(\tau) = \langle \xi(t)\xi(t+\tau)\rangle = \lim_{T\to\infty} \frac{1}{T}\int_{-T/2}^{T/2} \xi(t)\xi(t+\tau) dt. \quad (7)$$

Additionally, $S_\nu(f)$ is related to phase power spectral density by

$$S_\phi(f) = S_\nu(f)/f^2. \quad (8)$$

In the case that $\xi(t)$ represents the noise $\varepsilon_{2n}(t) - 2\varepsilon_n(t)$, then Eq. (6) provides a description of the frequency noise power spectral density induced by this term on the out-of-loop beat. Equation (6) will include the possible effects of correlated dynamics between $\varepsilon_{2n}(t)$ and $\varepsilon_n(t)$, which add in quadrature with the completely uncorrelated components of $\varepsilon_{2n}(t)$ and $\varepsilon_n(t)$. Thus, $S_\nu(f)$ of Eq. (6), with $\xi(t) = \varepsilon_{2n}(t) - 2\varepsilon_n(t)$, represents an upper limit to the completely uncorrelated noise between modes n and $2n$.

2. Experiment

The basic approach we take for our measurement of the out-of-loop coherence between modes n and $2n$ is to stabilize the comb to a CW laser, and then use the second harmonic of the same CW laser as a reference. When compared against the comb, this second harmonic reference enables the phase coherence of the comb across a full optical octave to be tested. The optical phase lock to the CW laser is implemented by servo control of the laser cavity length and pump power, while an f–$2f$ interferometer provides the additional signal used to stabilize f_0. The heterodyne beat between the comb and second harmonic CW reference represents the out-of-loop signal, which includes contributions from both the f_{rep} and f_0 phase locked loops as described by Eq. (5). Any differential-path effects limit the sensitivity of this measurement, and we have taken care to limit their effect by careful design.

The specific octave spanning Ti:sapphire frequency comb used in this experiment is similar to the system described in [24]. The relatively low repetition rate of 95 MHz leads to high pulse energy. This facilitates self phase modulation in the laser crystal, which broadens the spectrum to a full octave, the wings of which are not resonant with the cavity and are immediately transmitted by the output coupler. As detailed in Fig. 1, approximately 3 nm wide spectral regions at

#102990 - $15.00 USD Received 22 Oct 2008; revised 4 Dec 2008; accepted 12 Dec 2008; published 7 Jan 2009

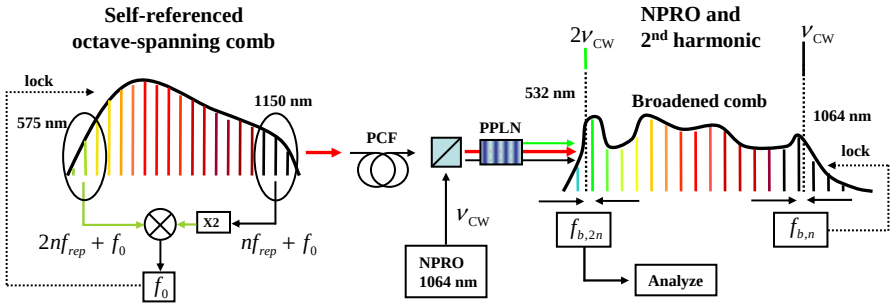

Fig. 1. After passing through an $f-2f$ interferometer for self-referencing, the remaining spectrum (600–1100 nm) from the octave-spanning frequency comb is broadened in photonic crystal fiber (PCF) and overlapped with the output of an NPRO Nd:YAG at 1064 nm. The resulting heterodyne beat, $f_{b,n}$, and the carrier envelope offset frequency, f_0, are locked to RF references. Polarization-selective doubling of the overlapped beams ensures that only the CW light is frequency doubled, while collinear beam propagation reduces technical noise. The out-of-loop beat at 532 nm, $f_{b,2n}$, is analyzed as detailed in the text.

575 nm and 1150 nm are used to measure f_0 with a standard f–$2f$ interferometer. This RF signal is used to lock f_0, via group delay actuation (using the same method as described in [22]), to an RF source that shares a common timebase with all the RF sources in the experiment. The remaining optical spectrum that is not used to measure f_0 consists of 600–1100 nm light, which is rebroadened to an optical octave centered near 750 nm using photonic crystal fiber (PCF). The output of the PCF is combined with a Nd:YAG non-planar ring oscillator (NPRO) CW optical reference at 1064 nm with polarization orthogonal to the comb. After passing through optical band-reject filters to remove the majority of the comb power in the unused central portion of the comb spectrum, the co-propagating comb and 500 mW of 1064 nm light pass through a temperature stabilized periodically poled lithium niobate (PPLN) crystal, doubling the 1064 nm CW light while overlapped with the comb, reducing technical noise due to differential path effects. The 1064 nm comb light is not doubled due to its orthogonal polarization, although if it were the resulting RF beat would be distinguishable from the true out-of-loop signal by its central frequency. A $\lambda/2$ at 1064 nm, λ at 532 nm wave plate is placed before the PPLN crystal in order to ensure that the the second harmonic CW light has the same polarization as the 532 nm comb light, since the PPLN outputs parallel polarizations of second harmonic and fundamental CW light. A single beam exits the PPLN crystal, with the 1064-nm comb light polarized orthogonally to the other three components of interest.

A Glan-Thompson polarizer separates the majority of the 1064 nm comb light and $\sim$1 mW of the CW 1064 nm light, allowing measurement of the RF heteredyne beat at 1064 nm. As described by Eqs. (2) and (3), this signal is used to stabilize the comb mode at ν_n ($n \simeq 3\times10^6$) by phase locking the heterodyne beat, via cavity length and pump power control, to an RF synthesizer. The remaining CW light at 1064 is transmitted by the polarizer, along with the majority of the comb and CW component at 532 nm.

The transmitted light contains approximately 500 μW of second harmonic CW light and comb near 532 nm, which is filtered to reject a large component of residual fundamental CW light. We measure the resulting heterodyne beat between the comb mode $2n$ and the second harmonic CW light. The expected RF frequency is given by Eq. (5), where ν_{CW} is now specifically referring to the frequency of the NPRO. In principle, the time-domain frequency error due to finite servo gain, given by

$$\delta f_{\rm lock}(t) = -\delta f_0(t) + 2\delta f_{b,n}(t), \tag{9}$$

#102990 - $15.00 USD Received 22 Oct 2008; revised 4 Dec 2008; accepted 12 Dec 2008; published 7 Jan 2009

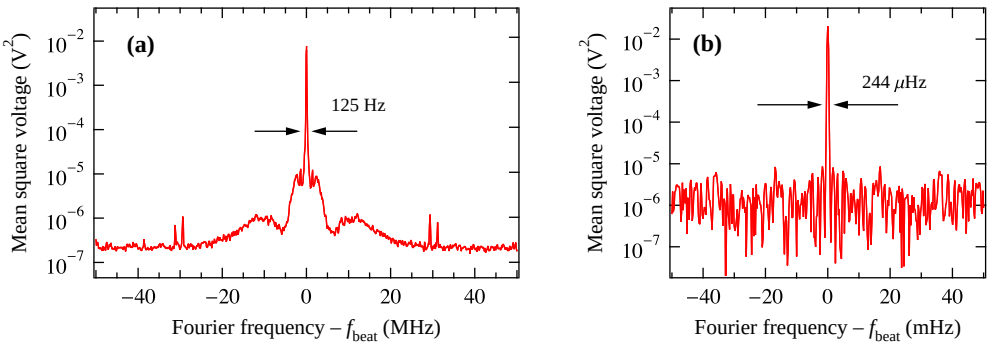

Fig. 2. **(a)** Out-of-loop beat mixed to 50 kHz at 100 kHz span with 125 Hz resolution bandwidth. Servo bumps are evident due to the contribution of finite locking gain and bandwidth to $\delta f_{\rm lock}(t)$. **(b)** Out-of-loop beat mixed to 1 Hz at 100 mHz span and 244 μHz resolution bandwidth. A strong coherent carrier is evident, even in this narrow resolution bandwidth.

can be estimated from the in-loop phase error signals and is indistinguishable from fundamental noise described by the term $\varepsilon_{2n}(t) - 2\varepsilon_n(t)$. The phase noise power spectral density associated with this term can be expressed via Eqs. (6–8) as

$$S_\phi(f) = \frac{4}{f^2}\int_0^\infty \cos(2\pi f\tau)\left[R_{\delta f_0\delta f_0}(\tau) + 4R_{\delta f_{b,n}\delta f_{b,n}}(\tau) - 4R_{\delta f_0\delta f_{b,n}}(\tau)\right]d\tau. \qquad (10)$$

If the cross-correlation term, $R_{\delta f_0\delta f_{b,n}}(\tau)$, is zero, the expected contribution of the locking error to the out-of-loop noise can thus be estimated by a weighted sum of the in-loop phase noise power spectral densities. This will only occur if there are no common noise sources for the servos locking f_0 and the comb to the NPRO reference.

While Eq. (10) gives a prediction for the out-of-loop frequency noise from the in-loop locking error, there are two additional important sources of out-of-loop noise that are indistinguishable from fundamental comb noise. Shot noise propagates through the optical phase locks for both $f_{b,n}$ and f_0, and adds in quadrature with the shot noise on the detector for $f_{b,2n}$, as discussed in Section 3. Out-of-loop technical noise such as differential path Doppler noise or amplitude to phase conversion in the PCF [25] also contributes to the measured out-of-loop phase noise spectrum.

One important feature of Eq. (5) is that it does not depend on the frequency of the NPRO, which, despite being quite stable due to its monolithic construction, has drifts on the order of 1 MHz/min. A shift of 1 MHz will show up on the 1 Hz level in $f_{b,m}(t)$ if $m = 2n+1$, *i.e.* the conjugate beat is used. This is clearly unacceptable for measuring comb linewidth on the μHz level. Thus, only $f_{b,2n}(t)$ is considered.

Figure 2 shows fast Fourier transforms (FFTs) of $f_{b,2n}(t)$, after it has been mixed down to near DC. Figure 2(b) represents the narrowest resolution bandwidth obtainable by the FFT instrument used in this experiment, due to an instrument-limited measurement time of ~ 1 hr. Obtaining better resolution bandwidth could be achieved by digitally sampling and recording the data over a longer time period and subsequently performing the FFT. However, at time scales over one hour, the microstructure fiber alignment drifts, causing the signal to noise ratio of the out-of-loop beat to drop well below 20 dB in a 100 kHz bandwidth. Servo unlocks also occur on this timescale due to finite servo range and thermal drift.

The measured single-sided phase noise spectral density of the out-of-loop beat, shown in

#102990 - $15.00 USD Received 22 Oct 2008; revised 4 Dec 2008; accepted 12 Dec 2008; published 7 Jan 2009

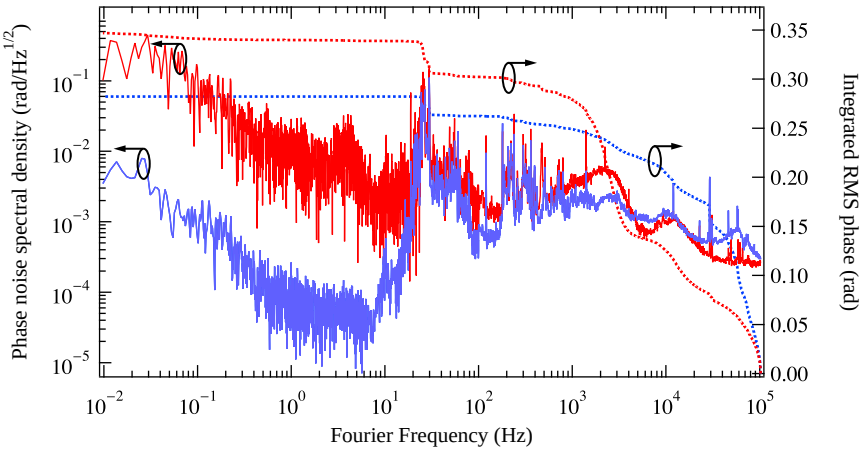

Fig. 3. Left axis: Estimate of the out-of-loop phase noise contribution of $\delta f_{\rm lock}$ based on a weighted incoherent sum of in-loop phase noise power spectral densities of both servo loops (blue) compared to the measured overall out-of-loop phase noise spectral density (red). Right axis: Root mean square (RMS) phase error integrated down from 100 kHz for both the contribution of the servo errors on out-of-loop noise (dashed blue) and the measured out-of-loop phase noise spectral density (dashed red).

Fig. 3, is complimentary to the linewidth measurement. The out-of-loop phase noise is directly visible in the sidebands of Fig. 2(a). We note that the integrated root-mean-square (RMS) phase is 0.35 rad when integrated down from 100 kHz to 10 mHz. This result, when combined with Fig. 2(b)—which shows no significant features 50 mHz away from the carrier—indicates that the 244 μHz instrument-limited coherent linewidth in Fig. 2(b) is a robust upper limit to the beat linewidth. The estimated locking error contribution to the phase noise from typical error signal spectral densities is additionally shown in Fig. 3. Here, Eq. (10) has been used with the assumption that $R_{\delta f_0 \delta f_{b,n}}(\tau) \rightarrow 0$. The discrepancy between the predicted out-of-loop phase noise near 50 kHz is due to the servo bump of the RF tracking filter used in the f_0 phase lock. The f_0 servo does not have the bandwidth to track this noise, so it appears only on the in-loop spectrum. Further discrepancies at Fourier frequencies in the 1 kHz range show the inadequacy of the assumption that $R_{\delta f_0 \delta f_{b,n}}(\tau) \rightarrow 0$, reflecting the fact that the cavity length and group delay servos are coupled when used to lock the comb to an optical reference and additionally may share common technical noise sources. When integrated from 100 kHz to 10 mHz, the expected integrated RMS phase predicted by the in-loop locking error is 70 mrad below the observed out-of-loop integrated phase error.

To overcome the measurement time-limited resolution bandwidth of 244 μHz and examine the out-of-loop beat at significantly improved phase noise sensitivity, we take the approach of studying the phase noise of a harmonic of the out-of-loop beat. A step recovery diode impedance matched at 100 MHz generates over 30 harmonics, amplifying the phase noise. The diode generates a $\sim$ 100 ps pulse for every high-to-low voltage zero crossing, and this output can be represented in the time domain as

$$V(t) = V_0 \sum_{k=-\infty}^{\infty} \Lambda\left[t - k/f_{\rm in} - \Delta\phi(t)/2\pi\right] \simeq V_0 \sum_{n=-\infty}^{\infty} a_n \exp\left[i2\pi n f_{\rm in} t - in\Delta\phi(t)\right]. \qquad (11)$$

Here, $\Lambda(t)$ is a temporally narrow function compared to the inverse input frequency, $f_{\rm in}$, and

#102990 - $15.00 USD Received 22 Oct 2008; revised 4 Dec 2008; accepted 12 Dec 2008; published 7 Jan 2009

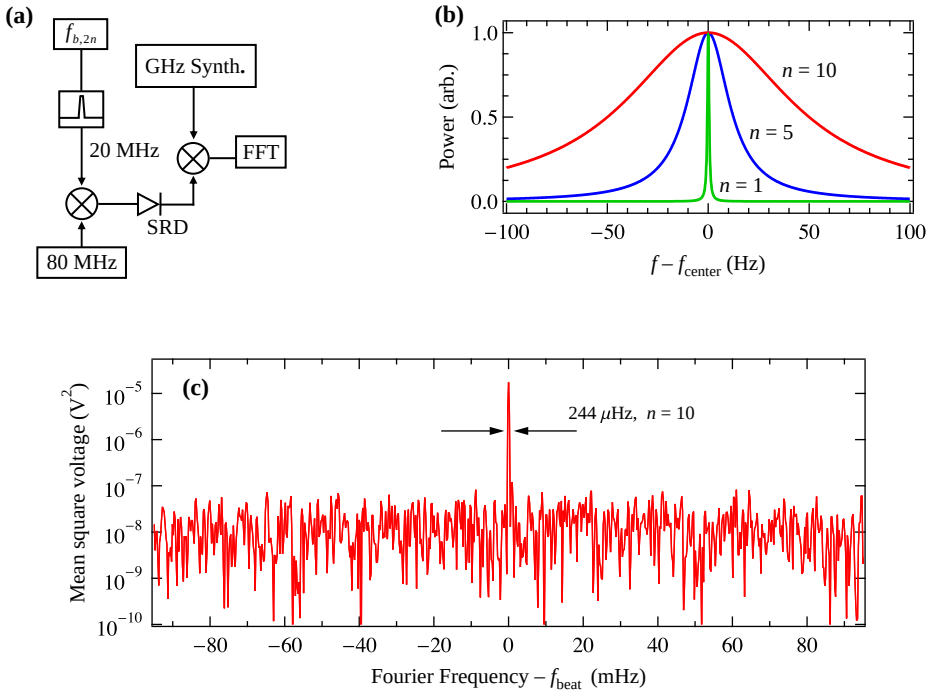

Fig. 4. **(a)** RF electronics for analyzing the tenth harmonic of the out-of-loop beat. The 20 MHz signal is filtered with a 2 kHz passband crystal filter and mixed to 100 MHz before being sent to the step-recovery diode (SRD). The tenth harmonic is selected for analysis. **(b)** Schematic depiction of a Lorentzian lineshape (green) broadened by frequency multiplication factors of $n = 5$ (blue) and $n = 10$ (red), yielding linewidths enhanced by a factor of 25 and 100, respectively. **(c)** Out-of-loop signal, 190 mHz span with a factor of 10 frequency multiplication. This corresponds to a 100-fold increase of the phase noise power spectral density in the vicinity of the carrier, resulting in a 100-fold increase in linewidth, yet a strong coherent peak is still observed in the 244 μHz resolution bandwidth.

a_k are the Fourier series coefficient for $\Lambda(t)$. The above approximation only holds if the phase can be approximated as stationary on the timescale of the envelope width. In the limit where $\Lambda(t)$ is a perfect Dirac delta function, Eq. (11) is exact. The final sum in Eq. (11) shows that for harmonic n the phase noise power spectral density, $S_\phi^n(f)$, is related to that of the fundamental, $S_\phi(f)$, by

$$S_\phi^n(f) = n^2 S_\phi(f). \tag{12}$$

In order to focus on the phase noise nearest the carrier, a narrow crystal filter centered at 20 MHz with a 2 kHz passband and 3 dB maximum ripple rejects phase and amplitude noise greater than 1 kHz away from the carrier. This further enforces the assumption of stationary phase noise on the time scale of $1/f_{\text{in}}$ and prevents broadband phase noise from causing carrier collapse when it is multiplied by the diode. Using the system whose key components are shown schematically in Fig. 4(a), we select the 10th harmonic of the step recovery diode and mix it down to near DC. Figure 4(c) shows the beat note is still resolution bandwidth limited, even with the 100-fold increase in phase noise power spectral density.

#102990 - $15.00 USD Received 22 Oct 2008; revised 4 Dec 2008; accepted 12 Dec 2008; published 7 Jan 2009

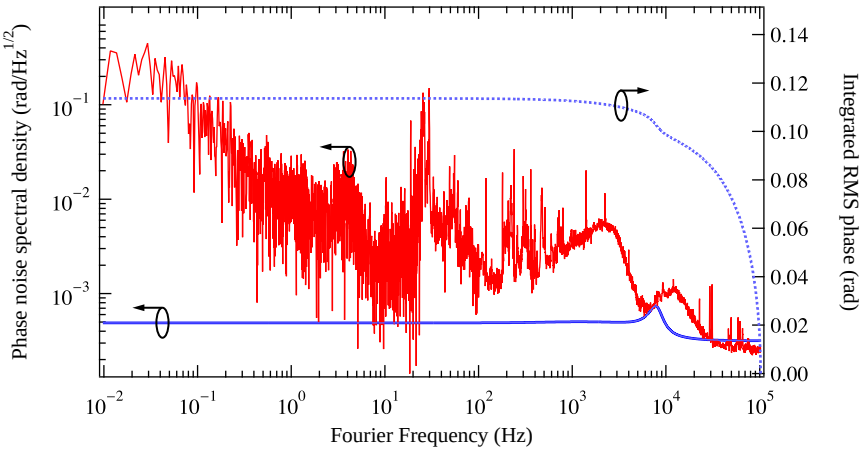

Fig. 5. Left axis: Estimated shot noise floor (blue) compared to the measured out-of-loop phase noise spectral density (red). Phase noise at Fourier frequencies above 12 kHz is limited by broadband light noise on the out-of-loop detector. Right axis: integrated root-mean-square (RMS) phase error from 100 kHz to 10 mHz for the estimated shot noise contribution (dashed blue).

3. Discussion

From Fig. 4(c), it is clear that there is no significant phase noise near the carrier. In order to use this measurement to extrapolate an upper limit to the actual non-instrument limited linewidth, we choose a functional form of the phase spectral density corresponding to a random walk in phase,

$$S_\phi(f) = \frac{C}{f^2}. \tag{13}$$

This type of phase diffusion is found due to spontaneous emission in laser systems, resulting in the famous Schawlow-Townes limit [26, 27] and would arise if the comb were limited by an "intrinsic linewidth" due to random-walk relative phase diffusion amongst comb modes. The optical power spectral density corresponding to this form of phase noise is a Lorentzian with full width at half maximum (FWHM) given by $\Delta\nu_{\mathrm{FWHM}} = \pi C$. Using Eq. (12), the FWHM of the nth harmonic of the step recovery diode, $\Delta\nu^n_{\mathrm{FWHM}}$, will thus be related to that of the first harmonic by

$$\Delta\nu^n_{\mathrm{FWHM}} = n^2 \Delta\nu_{\mathrm{FWHM}}. \tag{14}$$

This broadening effect is illustrated in Fig. 4(b). By applying this relationship to the Fourier-limited linewidth measurement of 244 μHz with multiplication factor $n = 10$, we can extrapolate an upper limit to the comb intrinsic linewidth of 2.44 μHz.

Figure 3 indicates that there is approximately a 70 mrad difference between the extrapolated integrated phase error and the measured integrated phase error. The extra $\sim$ 100 mrad in-loop integrated phase error between 100 kHz and 10 kHz that is due only to the RF tracking filter servo bump indicates that the true difference, which is an estimate of the total out-of-loop noise, is at least twice as large. The extra phase noise could come from technical sources, such as amplitude to phase conversion in the PCF [25] or differential-path Doppler noise. Fundamental noise sources that cause out-of-loop noise are shot noise and the noise term $\varepsilon_{2n}(t) - 2\varepsilon_n(t)$.

In order to estimate the effect of shot-noise limited detection on the out-of-loop beat, we consider the signal to noise ratio at each of the relevant detectors assuming shot-noise-limited detection. By modeling each servo using simple proportional-integral (PI) transfer functions

#102990 - $15.00 USD Received 22 Oct 2008; revised 4 Dec 2008; accepted 12 Dec 2008; published 7 Jan 2009

and using empirically determined gain and bandwidth coefficients for both the cavity length and group delay servos, we show in Fig. 5 the effect of shot noise on the out-of-loop beat. This noise floor is compared with the measured out-of-loop spectrum, indicating that below 30 kHz, the measurement is technical noise limited. This justifies the choice of a 100 kHz upper bound on the phase noise integration shown in Fig. 3. Under a sufficiently large servo bandwidth, the noise contribution due to Eq. (9) would ideally be eliminated, leaving the shot noise floor as the ultimate limit to the measurement's sensitivity to other noise sources, such as out-of-loop technical noise or intrinsic comb noise. As seen in Fig. 5, the total estimated integrated phase due to shot noise is of order 100 mrad.

While it is surprising that out-of-loop technical noise sources do not dominate the measured out-of-loop spectrum, it is important to note that many of the typical noise sources, such as differential path effects, were designed to be common-mode in our measurement. The results of [20] show that even without such careful design, the total effect of measurement noise does not inhibit sub-millihertz measurement precision. Beyond common mode cancelation, additional out-of-loop noise sources may be obscured due to other higher-order correlations amongst these processes.

In analogy to the Schawlow-Townes limit, the effect of spontaneous emission noise on frequency combs has been explored [28–31]. With spontaneous emission as the only quantum noise source, Paschotta *et al.* find quantum-induced timing jitter causes extra phase noise in the spectral wings [29]. Wahlstrand *et al.* take a more complete approach, considering all quantum noise drivers and empirically determined coupling coefficients to extrapolate the quantum-limited linewidth of individual comb modes as a function of frequency [31]. Both of these results are predictions of the spectral width of a comb mode compared to an outside reference, not between individual lines of the same comb. However, they are useful conceptual tools to understand the scale of the quantum noise. While a locked in-loop error signal linewidth can be measured to be arbitrarily small, it is the passive mode-locking mechanism that keeps the relative coherence of comb modes an octave away from being differentially affected by spontaneous emission noise. We obtain a conservative lower-limit for the free-running quantum-limited linewidth of our system from the result given by Paschotta *et al.*

$$\Delta\nu = \Delta\nu_{ST}\left[1 + (2\pi\delta\nu\tau_p)^2\right]. \tag{15}$$

Here, $\Delta\nu_{ST}$ is the result obtained by directly applying the Schawlow-Townes limit to the comb, $\delta\nu$ is the distance from the central frequency, and τ_p is the output pulse width. When we insert the relevant parameters, we obtain $\Delta\nu \simeq 100\mu$Hz for comb wavelengths near 1064 nm and 532 nm. The analysis of Wahlstrand *et al.* indicates that full consideration of noise coupling processes can result result in linewidths orders of magnitude larger in these spectral regions.

By observing a relative linewidth between comb lines an octave apart that is at least two orders of magnitude lower than that predicted for a free-running quantum-limited comb, we have shown that the mode-locking mechanism does an excellent job of correlating quantum-driven phase noise between two comb modes that are one octave apart. Even though only two degrees of freedom are controlled, the passive mode-locking process leads to a well-defined phase relationship across the visible and near-IR spectrum.

4. Conclusion

By carefully controlling sources of technical noise, we have placed a new limit on the phase coherence of an optical frequency comb by using second harmonic generation to compare modes n and $2n$. Phase noise measurements show a total RMS integrated optical phase error from 100 kHz to 10 mHz of 0.35 rad, and that the majority of accumulated phase error is due to finite

#102990 - $15.00 USD Received 22 Oct 2008; revised 4 Dec 2008; accepted 12 Dec 2008; published 7 Jan 2009

servo gains, not technical noise from the PCF or intrinsic noise from the comb. We have additionally placed limits on the fundamental phase-coherence of second harmonic generation, an extension of the results of Stenger *et al.* [19]. The relative linewidth of comb modes an octave apart is less than 2.5 μHz, with no significant phase noise features near the carrier, indicating that the mode-locking process strongly correlates quantum noise due to spontaneous emission across the comb. This result is at least two orders of magnitude below the predicted individual comb modes' quantum-limited linewidths. Thus, local phase perturbation due to spontaneous emission at a given wavelength is converted into a global phase perturbation, affecting all modes equally within the mode-locking bandwidth. The robust broadband phase coherence shown here demonstrates that there is essentially no practical limit to comb-facilitated coherent distribution of optical clock signals to arbitrary visible and near-IR wavelengths.

Acknowledgements

We thank J. Hall, S. Cundiff, J. Wahlstrand, and K. Cossel for their insightful input and discussions; and C. Menyuk for illuminating the effect of higher-order noise correlations on our results and a careful reading of the manuscript. This work is supported by DARPA, NIST, and NSF.

#102990 - $15.00 USD Received 22 Oct 2008; revised 4 Dec 2008; accepted 12 Dec 2008; published 7 Jan 2009